Stress Distribution Analysis of Novel Dental Mini-Implant Designs to Support Overdenture Prosthesis

Mariana Lima da Costa Valente, PhD[1]
Ana Paula Macedo, PhD[2]
Andréa Cândido dos Reis[3*]

This study aimed to test and compare 2 novel dental mini-implant designs to support overdentures with a commercial model, regarding the stress distribution, by photoelastic analysis. Three different mini-implant designs (Ø 2.0 mm × 10 mm) were tested: G1—experimental threaded (design with threads and 3 longitudinal and equidistant self-cutting chamfers), G2—experimental helical (design with 2 long self-cutting chamfers in the helical arrangement), and G3—Intra-Lock System. After including the mini-implants in a photoelastic resin, they were subjected to a static load of 100 N under two situations: axial and inclined model (30°). The fringe orders (n), that represents the intensity of stresses were analyzed around the mini-implants body and quantified using Tardy's method that calculates the maximum shear stress (τ) value in each point selected. In axial models, less stress was observed in the cervical third mini-implants, mainly in G1 and G2. In inclined models (30°), higher stresses were generated on the opposite side of the load application, mainly in the cervical third of G2 and G3. All mini-implant models presented lower tensions in the cervical third compared with the middle and apical third. The new mini-implants tested (G1 and G2) showed lower stresses than the G3 in the cervical third under axial load, while loading in the inclined model generated greater stresses in the cervical of G2.

Key Words: Biomechanics, dental implants, design, overdenture, photoelasticity

INTRODUCTION

The increasing prevalence of edentulism is associated with the aging population worldwide.[1] For many years, complete mandibular prostheses were the standard treatment to rehabilitate edentulous patients. Because of advances in implantology, many problems associated with conventional prostheses—such as lack of retention, stability, and the patient's discomfort—can be solved.[2–4]

In the presence of a narrow alveolar ridge, installing standard diameter implants requires a prior grafting procedure, often associated with an increased risk of morbidity, duration of treatment, and costs.[2–4] In these cases, implants with reduced diameter, less than 3 mm, or mini dental implants (MDIs), may represent a viable alternative, because they eliminate engraftment procedures on an alveolar ridge with reduced vestibular-lingual dimensions, allow installation with a flapless approach, present a simpler surgical technique, and are less costly for the patient.[5–10]

However, MDIs are subject to greater stresses due to the smaller surface area and volume of these implants, so that the per square mm load on the bone is increased by a factor of about 2×.[9,11] This can cause problems and complications related to its mechanical properties, such as deformation and fracture. Therefore, their length should be as anatomically as long as possible to compensate for the reduced diameter and provide adequate support to overdentures.[12]

In contrast with the higher stresses generated, the bone resorption caused by mini-implants might be reduced. The smaller circumference of the mini-implants can reduce the complications of peri-implant epithelial fixation, such as implant perimucositis or peri-implantitis, reducing percutaneous exposure and the possibility of marginal bone resorption.[13] Besides, the 1-piece implant configuration with the attachment ball, without the presence of gaps between prosthetic component and implant, reduces the colonization of microorganisms in this region,[6] which also favors the maintenance of bone tissue in height.[14,15]

The design (macrogeometry) of dental implants should be provided a biomechanical performance[16] capable of reducing stress at the bone/implant interface, mainly in the cervical region where the incidence of axial and nonaxial loads in high levels may cause marginal bone resorption, reducing the longevity of the implant and prosthetic rehabilitation.[17–22] The loading duration and dynamic load situations can induce marginal bone loss, interfering with the long-term prognosis of implants and biological tissue reaction.[23] Thus, the stress analysis is crucial to determine the ideal design characteristics in the development of a new implant model.

Photoelasticity is a laboratory test used to analyze the biomechanical performance of implant designs under various loading conditions.[19,24,25] It summarizes the stress distribution

[1] Department of Dental Materials and Prosthesis, School of Dentistry of Ribeirão Preto, University of São Paulo, Ribeirão Preto, Brazil. Av. do Café, s/n, 14040-904, Ribeirão Preto – SP, Brazil.
[2] Department of Dental Materials and Prosthesis, School of Dentistry of Ribeirão Preto, University of São Paulo, Ribeirão Preto, Brazil. Av. do Café, s/n, 14040-904, Ribeirão Preto – SP, Brazil.
[3] Department of Dental Materials and Prosthesis, School of Dentistry of Ribeirão Preto, University of São Paulo, Ribeirão Preto, Brazil. Av. do Café, s/n, 14040-904, Ribeirão Preto – SP, Brazil.
**Corresponding author,* e-mail: andreare73@yahoo.com.br
https://doi.org/10.1563/aaid-joi-D-19-00354

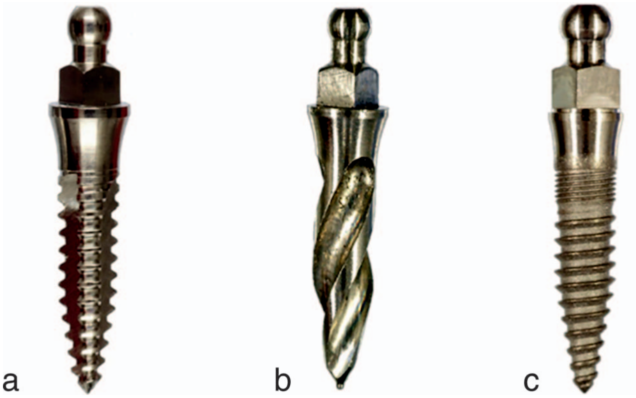

Figure 1. Dental mini-implants: (a) G1—Experimental threaded; (b) G2—Experimental helical; (c) G3—Intra-Lock.

behavior and characterizes the quality and quantity of stress through colored pattern known as isochromatic fringes when a load is applied. This effect results from the refraction of the polarized light by internal deformations because of stresses occurring in the model. Interpretation of these fringes shows the stress distribution and allows the measurement of their direction and magnitude. New implant designs are constantly launched in the dental market, to provide improvements and advances in the clinical success of implant prostheses.

Since stress distribution for the bone tissue is an important factor related to macrogeometry, this study aimed to test, by photoelastic analysis, the stress pattern generated by 2 experimental mini-implant models compared with a commercially available model.

Material and methods

Three acrylic master models were prepared (20 × 30 × 10 mm) according to the method used in previous studies.[21,24] A central and perpendicular drilling was performed in each model to include the mini-implants (Ø 2 mm × 10 mm): G1—Experimental threaded; G2—Experimental helical, and G3—MDL 2.010M (Intra-Lock System, Florida, USA) (Figure 1), positioned at the level model and fixed with a cyanoacrylate adhesive (Super Bonder, Henkel Loctite Sticker Ltda., São Paulo, SP, Brazil).

Two mini-implants were designed in Ti-6Al-4V, with dimensions of Ø 2 mm × 10 mm in length. The threaded model exhibited 3 longitudinal and equidistant self-cutting chamfers; the helical model exhibited 2 long self-cutting chamfers in the helical arrangement, similar to a drill. The commercial model MDL 2.010M (Ø 2 mm × 10 mm in length) (Intra-Lock System) was used as a comparison standard.

A silicone impression (Silicone Master, Talladium do Brazil, Curitiba, PR, Brazil) of the master's models was performed to correctly transfer the mini-implants to the photoelastic models. After obtaining the silicon matrix, the photoelastic resin (Araldite GY 279 and Aradur 2963, Araltec, Guarulhos, SP, Brazil) was prepared in the ratio 2:1 and was slowly poured into the silicon matrices. After polymerization, photoelastic models were sanded and polished to standardize the predetermined dimensions (20 × 30 × 10 mm) by wet sanding.

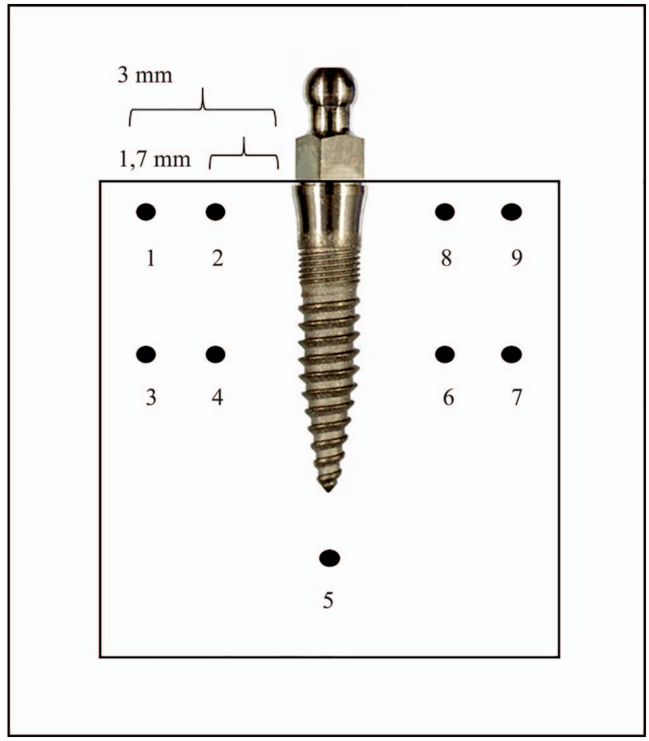

Figure 2. Draft of the position of the points analyzed.

Qualitative analysis

For the analysis, the models' photoelastic experiments were performed using a flat transmission polariscope, model FL200, G.U.N.T. (Gerätebau GmbH, Barsbuettel, Germany), with a Cyber-shot DSC-HX100V digital camera, (Sony, Tokyo, Japan) attached to a tripod and positioned in front of the device to record situations of interest. An Universal Testing Machine (EMIC-DL 10000, São José dos Pinhais, São Paulo, Brazil) with a load cell of 50 kgf was used for load application of 100 N. The load (100 N) was applied in two situations: (1) axial model; and (2) inclined model (30°).

Before analysis in polariscope, each photoelastic model was subjected to thermal stress relaxation (50°C for 10 min + 10 min cooling at ~ 22° C)[21,24] to certify the absence of residual stresses. The images obtained were analyzed and the intensity and location of the stresses were subjectively compared, through a colorful spectrum where the fringe order 0 corresponds to black; 1 violet/blue transition; 2 purple/blue transition; and 3 red/green transition.

Quantitative analysis

Nine points of interest around the mini-implant body were selected: 4 in the cervical, 4 in the middle, and 1 in the apical third (Figure 2). The maximum shear stress (τ) values (KPa) in each point were measured using Tardy's compensation method, represented by the following equation: $\tau = (n \times K)/(2 \times b)$. Where (n) is the value of the fringe order at the analyzed point; (K) is the optical constant of the photoelastic resin (3.56 Brewsters),[24] and (b) is the photoelastic model thickness in millimeters (mm).

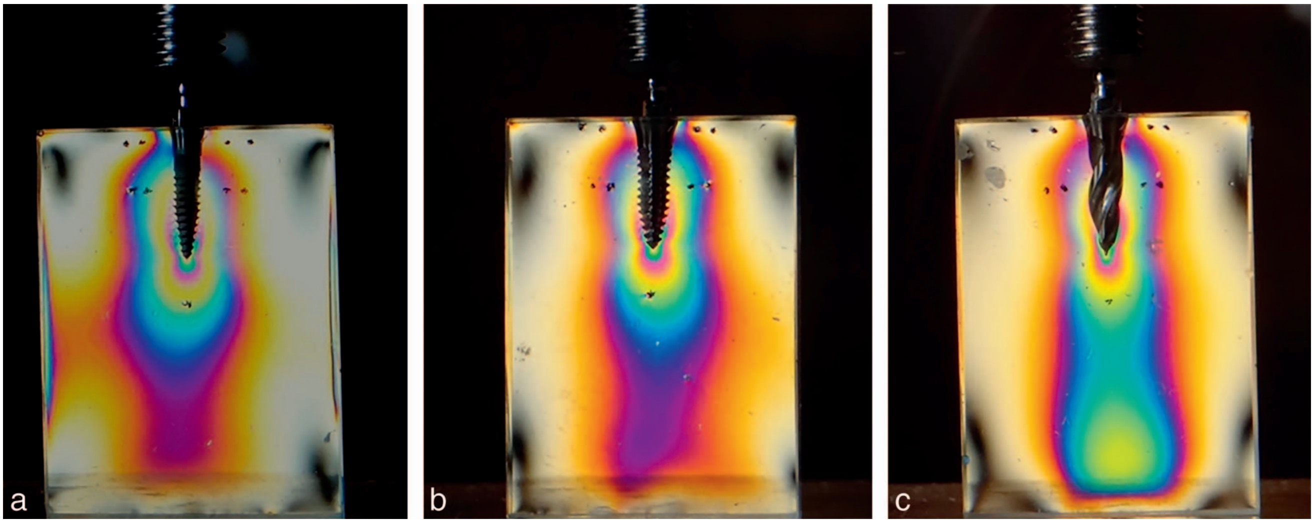

Figure 3. Stresses resulting from load application (axial model): (a) G1—Experimental threaded; (b) G2—Experimental helical; (c) G3—Intra-Lock.

Results

The intensity of the stresses represented through the fringe order was analyzed in the different points of each model (Figure 2). In this study, applying 100 N load in axial models promotes fringe orders 0 in the cervical third (points 1–2 and 8–9) of all groups of mini-implants (G1, G2, and G3). In the middle third (points 3–4 and 6–7), fringe orders 0 and 1 were visualized in all designs of mini-implants (G1, G2, and G3), and in the apical third (point 5), fringe orders 1 were observed in all groups (Figure 3) (Table 1).

The application of 100 N load in the inclined models (30°) showed a predominance of stresses on the opposite side of the loading. In the cervical third (points 1–2), higher stresses, fringe order 2, were observed in G2 and G3. In the middle third (points 3–4), stresses were similar for all mini-implants, and in the apical third (point 5), the highest stress was observed in G2 (Figure 4) (Table 2).

Table 1

Fringe order (N) and Stress (kPa) in each point analyzed, in the axial models G1, G2, and G3

	G1		G2		G3	
Points	Fringe Order	Stress	Fringe Order	Stress	Fringe Order	Stress
1	0.264	39.3	0.292	43.4	0.539	80.2
2	0.500	74.4	0.472	70.2	0.683	101.6
3	0.744	110.7	0.742	110.3	1.033	153.7
4	0.989	147.1	0.783	116.5	1.178	175.2
5	1.233	183.5	1.228	182.6	1.250	185.9
6	1.156	171.9	1.128	167.8	0.772	114.9
7	0.842	125.2	0.828	123.1	0.628	93.4
8	0.600	89.3	0.567	84.3	0.500	74.4
9	0.419	62.4	0.406	60.3	0.353	52.5

Discussion

The stress distribution significantly influences the longevity of implant-supported rehabilitations.[11] Material, type of prosthesis, and implant design are the major factors involved in this process.[11] Although mandibular overdentures are well-established as a treatment option for edentulous patients, the main complications occur when the stress generated by masticatory loads exceeds the physiological limit of the bone tissue, starting the process of resorption and appearance of microfractures at the bone-implant interface.[19,25,26]

Residual ridge resorption, presence of systemic complications, and high costs are the major limitation of rehabilitation with standard diameter implants, despite the great technical-scientific development and benefits offered by this technique.[27] The development of new implant designs that offer simplified and less invasive surgical techniques, faster patient recovery, and lower costs for the patients still represent a need for oral rehabilitation with implants and has the potential to expand the indications of this treatment modality, especially for edentulous patients.[28] However, to validate the effectiveness of new designs, some parameters must be extensively investigated. Therefore, this study aimed to test the stress distribution in 2 experimental mini-implant designs, compared with a commercially available model, under different loading conditions.

The preservation of the bone crest and peri-implant tissues is essential for the success of rehabilitation with implants.[18,20,29,30] The highest concentration of tensions and consequent bone resorption occurs in the cervical region; however, in this study, mini-implant models exhibited lower tensions in this region, with a predominance of fringes of order 0, which corresponds to the absence of tensions. This probably occurred for the geometric characteristics and diameter of the tested designs, which shows a favorable result under the application of axial load.

The implant parameters that influence the load transfer to

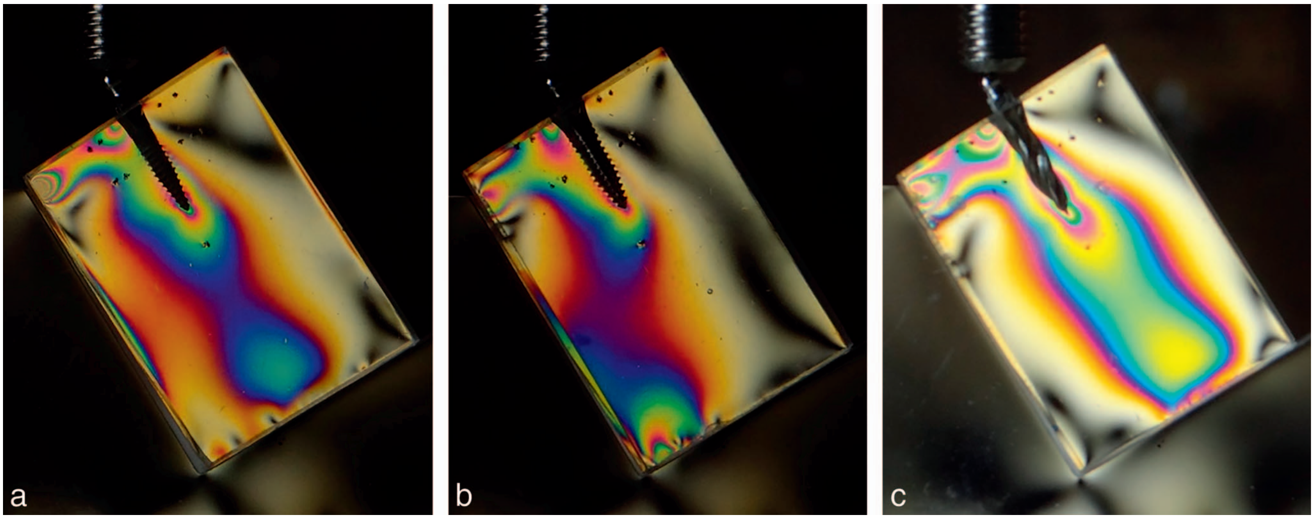

Figure 4. Stresses resulting from load application (inclined model-30°): (a) G1—Experimental threaded; (b) G2—Experimental helical; (c) G3—Intra-Lock.

the bone tissue are related to the diameter and length and, with threaded implants, the thread pitch, its shape, and depth.[31] These are reasons we have observed higher stresses in the middle third of the tested mini-implants, because of design changes in that region, such as the presence of longitudinal cutting chamfers in G1, and greater thread pitch and helical configuration in G2.

As observed in other studies by photoelastic analysis,[29,32,33] the present study also showed that the application of the oblique load promotes a higher concentration of stresses on the opposite side of the load application. It can be explained by implant angulation that generates a greater lever arm during loading application and promotes higher torque around the implant.[34]

Intra-Lock and helical mini-implants showed higher stresses in the cervical third. These results corroborate the literature data, which associate higher stresses in the cervical region of the implants in the presence of oblique forces, which can lead to bone resorption, fracture of prosthetic components, and impairment of rehabilitation treatment. According to a previous study,[35] for example, oblique forces result in stress at the bone crest 5 times higher compared with axial loading. These findings confirm that nonaxial forces increases stress in the cervical region[22] and can lead to bone resorption and even fracture of the mini-implants. Therefore, the prosthesis/implant biomechanical system must be balanced, avoiding stress concentration.

The factors affecting the load transfer at the bone-implant interface include the type of loading, material properties of implant and prosthesis, implant geometry, surface structure, quality and quantity of the surrounding bone, and the nature of the bone-implant interface.[36] Regarding the influence of design, the new mini-implants analyzed, threaded, and helical, showed similar stress distribution to the commercial model tested; however, non-axial forces induces higher stress on the cervical third. Thus, to avoid marginal bone resorption and implant failure, it is necessary to ensure a biomechanically controlled occlusion that can promote a uniform distribution of stress under different load conditions.

Table 2

Fringe order (N) and Stress (kPa) in each point analyzed, in the inclined models (30°) G1, G2, and G3

	G1		G2		G3	
Points	Fringe Order	Stress	Fringe Order	Stress	Fringe Order	Stress
1	1.256	186.8	2.000	297.5	1.672	248.7
2	1.689	251.2	2.428	361.1	2.006	298.3
3	1.228	182.6	1.061	157.8	1.083	161.1
4	1.533	228.1	1.347	200.4	1.356	201.6
5	1.044	155.4	1.522	226.4	1.261	187.6
6	0.233	34.7	0.703	104.5	0.347	51.6
7	0.106	15.7	0.531	78.9	0.183	27.3
8	0.417	62.0	0.367	54.5	0.394	58.7
9	0.472	70.2	0.333	49.6	0.411	61.2

Conclusion

In this study, the photoelastic analysis showed that all models of mini-implants had lower stresses in the cervical third compared to the middle and apical thirds. Concerning the mini-implants tested the new designs (G1 and G2) showed less stress in the cervical third, under axial load, compared to G3. The inclination of the models by 30° generated higher stress in the cervical third of G2.

Abbreviations

G1: Group 1
G2: Group 2
G3: Group 3
MDIs: mini-dental implants

Acknowledgments

This work was supported by the Foundation for Research Support of the State of São Paulo [grant numbers 2014/27362-2]. The authors declare no potential conflicts of interest with respect to the authorship and/or publication of this article.

References

1. Reissmann DR, Dard M, Lamprecht R, Struppek J, Heydecke G. Oral health-related quality of life in subjects with implant-supported prostheses: a systematic review. *J Dent*. 2017;65:22–40.

2. Abraham CM. A brief historical perspective on dental implants, their surface coatings and treatments. *Open Dent J*. 2014;8:50–55.

3. AlZarea BK. Oral health related quality-of-life outcomes of partially edentulous patients treated with implant-supported single crowns or fixed partial dentures. *J Clin Exp Dent*. 2017;9:666–671.

4. Valente ML, de Castro DT, Shimano AC, Lepri CP, dos Reis AC. Analyzing the influence of a new dental implant design on primary stability. *Clin Implant Dent Relat Res*. 2016;18:168–173.

5. Elsyad MA, Gebreel AA, Fouad MM, Elshoukouki AH. The clinical and radiographic outcome of immediately loaded mini implants supporting a mandibular overdenture. A 3-year prospective study. *J Oral Rehabil*. 2011;38: 827–834.

6. Flanagan D, Mascolo A. The mini dental implant in fixed and removable prosthetics: a review. *J Oral Implantol*. 2011;37:123–132.

7. Takagaki K, Gonda T, Maeda Y. Number and location of mini-implants retaining a mandibular overdenture to resist lateral forces: a preliminary in vitro study. *Int J Prosthodont*. 2017;30:248–250.

8. Preoteasa E, Imre M, Preoteasa CT. A 3-year follow-up study of overdentures retained by mini-dental implants. *Int J Oral Maxillofac Implants*. 2014;29:1170–1176.

9. Elsyad MA. Patient satisfaction and prosthetic aspects with mini-implants retained mandibular overdentures. A 5-yearprospective study. *Clin Oral Implants Res*. 2016;27:926–933.

10. Warin P, Rungsiyakull P, Rungsiyakull C, Khongkhunthian P. Effects of different numbers of mini-dental implants on alveolar ridge strain distribution under mandibular implant-retained overdentures. *J Prosthodont Res*. 2018;62:35–43.

11. Sallam H, Kheiralla LS, Aldawakly A. Microstrains around standard and mini implants supporting different bridge designs. *J Oral Implantol*. 2012;38:221–229.

12. Lemos CA, Verri FR, Batista VE, Júnior JF, Mello CC, Pellizzer EP. Complete overdentures retained by mini implants: a systematic review. *J Dent*. 2017;57:4–13.

13. Flanagan D. Rationale for definitive mini dental implant treatment. *J Oral Implantol*. 2021; 47:437–444.

14. Pita MS, Anchieta RB, Barão VA, Garcia IR Jr, Pedrazzi V, Assunção WG. Prosthetic platforms in implant dentistry. *J Craniofac Surg*. 2011;22: 2327–2331.

15. Gurgel-Juarez NC, de Almeida EO, Rocha EP, et al. Regular and platform switching: bone stress analysis varying implant type. *J Prosthodont*. 2012;21:160–166.

16. Ozkir SE, Terzioglu H. Macro design effects on stress distribution around implants: a photoelastic stress analysis. *Indian J Dent Res*. 2012;23: 603–607.

17. Ishigaki S, Nakano T, Yamada S, Nakamura T, Takashima F. Biomechanical stress in bone surrounding and implant under simulated chewing. *Clin Oral Implants Res*. 2003;14:97–102.

18. Zanatta LC, Dib LL, Gehrke SA. Photoelastic stress analysis surrounding different implant designs under simulated static loading. *J Craniofac Surg*. 2014;25:1068–1071.

19. Gehrke SA, Frugis VL, Shibli JA, et al. Influence of implant design (cylindrical and conical) in the load transfer surrounding long (13 mm) and short (7 mm) length implants: a photoelastic analysis. *Open Dent J*. 2016;10: 522–530.

20. Mohammed Ibrahim M, Thulasingam C, Nasser KS, Balaji V, Rajakumar M, Rupkumar P. Evaluation of design parameters of dental implant shape, diameter and length on stress distribution: a finite element analysis. *J Indian Prosthodont Soc*. 2011;11:165–171.

21. Aguiar FA Jr, Tiossi R, Macedo AP, Mattos Mda G, Ribeiro RF, Rodrigues RC. Photoelastic analysis of stresses transmitted by universal cast to long abutment on implant-supported single restorations under static occlusal loads. *J Craniofac Surg*. 2012;23:2019–2023.

22. de Castro Ferreira E, Corbella S, Zanatta LC, Taschieri S, del Fabbro M, Gehrke SA. Photo-elastic investigation of influence of dental implant shape and prosthetic materials to patterns of stress distribution. *Minerva Stomatol*. 2012;61:263–272.

23. Solberg K, Heinemann F, Pellikaan P, et al. Finite element analysis of different loading conditions for implant-supported overdentures supported by conventional or mini implants. *Comput Methods Biomech Biomed Engin*. 2017;20:770–782.

24. Valente MLDC, de Castro DT, Macedo AP, Shimano AC, Dos Reis AC. Comparative analysis of stress in a new proposal of dental implants. *Mater Sci Eng C Mater Biol Appl*. 2017;77:360–365.

25. Zaparolli D, Peixoto RF, Pupim D, Macedo AP, Toniollo MB, Mattos MDGC. Photoelastic analysis of mandibular full-arch implant-supported fixed dentures made with different bar materials and manufacturing techniques. *Mater Sci Eng C Mater Biol Appl*. 2017;81:144–147.

26. Okumura N, Stegaroiu R, Kitamura E, Kurokawa K, Nomura S. Influence of maxillary cortical bone thickness, implant design and implant diameter on stress around implants: a three-dimensional finite element analysis. *J Prosthodont Res*. 2010;54:133–142.

27. Marcello-Machado RM, Faot F, Schuster AJ, Nascimento GG, Del Bel Cury AA. Mini-implants and narrow diameter implants as mandibular overdenture retainers: a systematic review and meta-analysis of clinical and radiographic outcomes. *J Oral Rehabil*. 2018;45:161–183.

28. Goiato MC, Shibayama R, Gennari Filho H, et al. Stress distribution in implant-supported prostheses using different connection systems and cantilever lengths: digital photoelasticity. *J Med Eng Technol*. 2016;40:35–42.

29. Zanardi PR, Stegun RC, Sesma N, Costa B, Shibli JA, Laganá DC. Stress distribution around dental implants placed at different depths. *J Craniofac Surg*. 2015;26:2163–2166.

30. Lee JI, Lee Y, Kim YL, Cho HW. Effect of implant number and distribution on load transfer in implant-supported partial fixed dental prostheses for the anterior maxilla: a photoelastic stress analysis study. *J Prosthet Dent*. 2016;115:161–169.

31. Lan TH, Du JK, Pan CY, Lee HE, Chung WH. Biomechanical analysis of alveolar bone stress around implants with different thread designs and pitches in the mandibular molar area. *Clin Oral Investig*. 2012;16:363–369.

32. Pellizzer EP, Carli RI, Falcón-Antenucci RM, Verri FR, Goiato MC, Villa LM. Photoelastic analysis of stress distribution with different implant systems. *J Oral Implantol*. 2014;40:117–122.

33. Rasouli-Ghahroudi AA, Geramy A, Yaghobee S, et al. Evaluation of platform switching on crestal bone stress in tapered and cylindrical implants: a finite element analysis. *J Int Acad Periodontol*. 2015;17:2–13.

34. Sennerby L, Rocci A, Becker W, Jonsson L, Johansson LA, Albrektsson T. Short-term clinical results of Nobel Direct implants: a retrospective multicentre analysis. *Clin Oral Implants Res*. 2008;19:219–226.

35. Goiato MC, Pesqueira AA, Santos DM, Haddad MF, Moreno A. Photoelastic stress analysis in prosthetic implants of different diameters: mini, narrow, standard or wide. *J Clin Diagn Res*. 2014;8:86–90.

36. Bourauel C, Aitlahrach M, Heinemann F, Hasan I. Biomechanical finite element analysis of small diameter and short dental implants: extensive study of commercial implants. *Biomed Tech (Berl)*. 2012;57:21–32.